CHEMISTRY
A EUROPEAN JOURNAL

DOI: 10.1002/chem.200801206

Intramolecular Charge Interactions as a Tool to Control the Coiled-Coil-to-Amyloid Transformation

Kevin Pagel,[a] Sara C. Wagner,[a] Raheleh Rezaei Araghi,[a] Hans von Berlepsch,[b] Christoph Böttcher,[b] and Beate Koksch*[a]

Dedicated to Professor Michael Bienert on the occasion of his 65th birthday

Abstract: Under the influence of a changed environment, amyloid-forming proteins partially unfold and assemble into insoluble β-sheet rich fibrils. Molecular-level characterization of these assembly processes has been proven to be very challenging, and for this reason several simplified model systems have been developed over recent years. Herein, we present a series of three de novo designed model peptides that adopt different conformations and aggregate morphologies depending on concentration, pH value, and ionic strength. The design strictly follows the characteristic heptad repeat of the α-helical coiled-coil structural motif. In all peptides, three valine residues, known to prefer the β-sheet conformation, have been incorporated at the solvent-exposed b, c, and f positions to make the system prone to amyloid formation. Additionally, pH-controllable intramolecular electrostatic repulsions between equally charged lysine (peptide A) or glutamate (peptide B) residues were introduced along one side of the helical cylinder. The conformational behavior was monitored by circular dichroism spectroscopic analysis and thioflavin T fluorescence, and the resulting aggregates were further characterized by transmission electron microscopy. Whereas uninterrupted α-helical aggregates are found at neutral pH, Coulomb repulsions between lysine residues in peptide A destabilize the helical conformation at acidic pH values and trigger an assembly into amyloid-like fibrils. Peptide B features a glutamate-based switch functionality and exhibits opposite pH-dependent folding behavior. In this case, α-helical aggregates are found under acidic conditions, whereas amyloids are formed at neutral pH. To further validate the pH switch concept, peptide C was designed by including serine residues, thus resulting in an equal distribution of charged residues. Surprisingly, amyloid formation is observed at all pH values investigated for peptide C. The results of further investigations into the effect of different salts, however, strongly support the crucial role of intramolecular charge repulsions in the model system presented herein.

Keywords: α–β structural transitions · amyloids · coiled-coil folding · protein models · self-assembly

Introduction

The formation of insoluble proteinaceous amyloid deposits is a common hallmark of many neurodegenerative diseases such as Alzheimer's disease, Parkinson's disease, and the transmissible spongiform encephalopathies.[1,2] Various non-disease related proteins have also recently been shown to aggregate into similar fibrillar structures under in vitro conditions, thus suggesting that the amyloid structure is a general feature of peptides and proteins.[2,3] Although amyloid-forming proteins do not usually possess sequence homologies, impressive structural similarities, such as an unbranched morphology, diagnostic dye binding, and a characteristic X-ray diffraction pattern, are found for their fibrillar assemblies.[4–6] The soluble forms of the involved proteins

[a] Dr. K. Pagel,[+] S. C. Wagner,[+] R. Rezaei Araghi, Prof. Dr. B. Koksch
Institute of Chemistry and Biochemistry
Freie Universität Berlin
Takustrasse 3, 14195 Berlin (Germany)
Fax: (+49) 30-838-55-644
E-mail: koksch@chemie.fu-berlin.de

[b] Dr. H. von Berlepsch, Priv.-Doz. Dr. C. Böttcher
Research Centre for Electron Microscopy
Freie Universität Berlin
Fabeckstrasse 36a, 14195 Berlin (Germany)

[+] These authors contributed equally to this work.

Supporting information for this article is available on the WWW under http://dx.doi.org/10.1002/chem.200801206.

mostly exhibit unfolded or partially α-helical conformations, whereas their insoluble amyloid analogues are rich in β-sheets. Consequently, a conformational transition has to take place before or during the assembly process. It is widely accepted that these structural transitions can be triggered by alterations of the environment, such as changes in pH value, ionic strength, or the presence of metal ions. However, the underlying molecular mechanisms remain unresolved to date, which might be a result of the extraordinary complexity of the molecular interactions and the challenging physicochemical properties of naturally occurring amyloid-forming systems.[7] Especially the low solubility, the limited order of fibrils, and mostly poor synthetic accessibility restrict the spectrum of analytical techniques and complicate characterization on a molecular level. To overcome these drawbacks, much effort has been spent in the last decade on the development of suitable and simplified model systems.[8]

Amyloid model systems in general are usually optimized for a certain purpose or application. Therefore, they may differ widely regarding size and complexity.[8] To investigate the impact of a changed environment on the underlying conformational transition, a well-defined initial conformation that mimics the native state of the protein is required. Following this idea, model systems based on the α-helical coiled-coil folding motif evolved as one of the most suitable approaches. The advantages are obvious: Coiled coils are very common in nature, the structure has been studied extensively, the design principles are very well understood, and the folding is based on oligomerization that is also the foundation for amyloid formation.[9–11] Several attempts to merge structural features of α-helical coiled coils and amyloids have been reported. In an early study, Mihara and co-workers, for example, used interactions between large hydrophobic groups attached to the N-terminus of a covalently linked coiled-coil dimer to provoke the assembly into amyloids.[12,13] Later, Woolfson and co-workers utilized a temperature increase to induce amyloid formation of a peptide that contained sequence features for both α-helical coiled coils and β-hairpin folding.[14] Further investigations that applied sequence modifications and elevated temperatures to trigger a coiled-coil-to-amyloid transformation have been reported by the groups of Kammerer and Hartgerink.[15–17] However, despite the enormous number of studies, relatively little is known about the molecular details of temperature-induced amyloid assembly processes. Elevated temperatures doubtlessly destabilize the α-helical coiled-coil conformation, but it is still unclear if this temperature increase is accompanied by a change in the overall hydrophobicity of the system.

In contrast to the above-mentioned strategies, we recently showed that structural conversions in coiled-coil-based amyloid-forming model peptides can also be initiated without non-natural building blocks or thermal activation. In these systems either the presence of metal ions[18] or changes in concentration and pH value[19] were shown to trigger conformational transitions in either direction. The sensitivity towards metal ions was realized by incorporation of two histidine residues at different positions within the coiled coil.[18] In contrast, sensitivity to the pH value was achieved by an accumulation of positively charged lysine residues at one side of the helical cylinder.[19] Protonation of these residues at acidic pH values results in the formation of an excessively charged domain, which induces an association into amyloid-like structures, whereas non-amyloidogenic coiled-coil assemblies have been obtained under neutral conditions. Herein, we provide additional experimental data and expand the idea of such intramolecular charge repulsions as tools to trigger conformational transitions and amyloid formation by changes in pH value and concentration. Two additional coiled-coil-based model peptides have therefore been designed and characterized regarding folding behavior and aggregate morphology. A comparison to the previous system revealed that subtle differences in the distribution of charged residues can yield specific pH-dependent conformational preferences. Variations in the ionic strength have furthermore been used to prove the role of excessively charged domains as a conformational trigger.

Results and Discussion

Design: The design of the presented model peptides is based on the well-known, naturally occurring α-helical coiled-coil folding motif. In general, coiled coils consist of two to five amphiphilic α-helices that are wound around one another with a slight left-handed superhelical twist.[9–11] The primary structure is characterized by a periodic repeat of seven residues, the so-called 4–3 heptad repeat, which is commonly denoted from a to g (Figure 1a). Positions a and d are typically occupied by nonpolar residues that form the first recognition motif by a distinctive hydrophobic core packing. Charged amino acids, such as glutamate, lysine, and arginine, at positions e and g form the second recognition motif by interhelical ionic interactions. For the model peptides presented herein, both coiled-coil recognition motifs have been designed to deliver maximized stability. Therefore, positions a and d were equipped with leucine residues, which ensure an efficiently packed hydrophobic core, whereas positions e and g were designed to form exclusively attractive electrostatic interactions between the helices in case of a parallel folding (Figure 1, frame).

The remaining positions b, c, and f within the heptad repeat are exposed to the solvent and do not contribute significantly to the coiled-coil oligomerization. Therefore, these positions are suitable for the incorporation of modifications without affecting the intrinsic ability of the system to adopt an α-helical coiled-coil conformation. Characteristic features of other structural motifs can be implemented here to generate a direct competition between two different conformations, the α-helical coiled coil and the β-sheet rich amyloid-like structure.

For the design presented herein, two different types of modification have been implemented into the idealized 26-residue coiled-coil model peptide. First, β-sheet-preferring

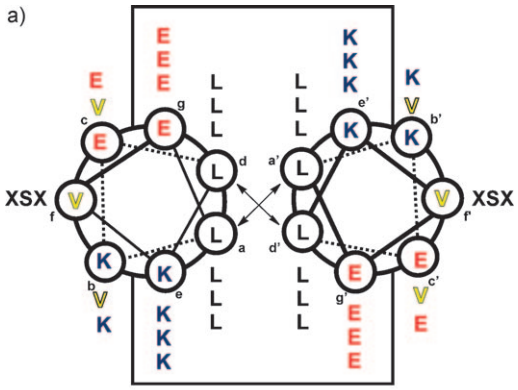

Figure 1. a) Helical-wheel presentation and b) sequences of the coiled-coil-based model peptides A (formerly denoted VW19 in ref. [19]), B, and C. Frame: Positions that induce the α-helical coiled-coil structure. Blue, red: Accumulation of equally charged residues that destabilize the α-helical structure under acidic or basic conditions, respectively. Yellow: Solvent-exposed valine residues make the system prone to amyloid formation. All the peptides were N-terminally labeled with anthranilic acid (Abz) for photometric concentration determination.

amino acids have been incorporated at the solvent-exposed coiled-coil positions to enhance the overall amyloid-formation propensity of the system (Figure 1, yellow). Preliminary investigations revealed that three valine residues at the positions b, c, and f are sufficient to make the system prone to amyloid formation, whereas the general ability for a helical folding is maintained (unpublished results). However, the tendency to assemble into fibrils was not or only insufficiently tunable. To overcome these problems, that is, to specifically direct the preference to a certain folding, conformational switches have been implemented as a second modification.

Different types of conformational switches[20] turned out to be suitable for our coiled-coil-based amyloid model. Recently, we showed that Cu^{2+}- and Zn^{2+}-dependent structural switches can be used to control the intrinsic tendency of the system to assemble into amyloids.[18] In that study, the relative positions of the metal-binding residues and the unique binding properties of the metal were shown to dictate folding. Besides this finding, previous investigations on a peptide termed VW19 revealed that pH-dependent conformational switches can efficiently be used to direct the conformational preferences of the system.[19] Therefore, the coiled-coil model system was equipped with positively charged lysine residues that generate an extended positively charged domain on one side of the helical cylinder. Under acidic conditions and concentrations above 300 μM, VW19 formed typical amyloid-like fibrils, whereas α-helical fibers were observed at neutral pH and comparable concentrations. On the basis of these results, we concluded that intramolecular Coulomb repulsions between lysine residues at acidic pH values destabilize the α-helical coiled coil and, as a consequence, shift the equilibrium to the competing amyloid form. In other words, if the pH switch is in the ON state under acidic conditions, the coiled coil is destabilized and the competing amyloid form takes control, whereas stable α-helical coiled-coil assemblies are formed by the pH switch in the OFF state at a neutral pH value. Two analogues of VW19 (henceforth denoted peptide A) were designed to further validate the concept of charge interactions for controlling the conformation of the system by pH value. The sequences of peptides A, B, and C are shown in Figure 1.

Peptide A contains eight lysine residues at positions b, e, and f that form the excessively charged domain. For peptide B, two lysine residues at position f were replaced by glutamic acid. As a consequence, an excess of eight negatively charged glutamate residues at positions c, f, and g now forms and a somewhat complementary behavior to peptide A may be expected from the design. To further elucidate the role of the overall charge excess that is present in peptides A and B, peptide C was modified with two neither positively nor negatively charged serine residues at the corresponding f positions. In contrast to peptides A and B, peptide C carries a balanced amount of acidic and basic side chains and, consequently, no excessively charged domain that provides pH sensitivity is present.

The design of model peptides A, B, and C can be summarized as follows: 1) Hydrophobic leucine residues at positions a and d in combination with interhelical electrostatic attractions between glutamate and lysine residues at positions e and g enable stable α-helical coiled-coil folding; 2) three valine residues at positions b, c, and f make the system prone to amyloid formation without affecting the general ability for a coiled-coil assembly; 3) positions b/e and c/g are occupied with equally charged residues in all peptides. Lysine and glutamic acid residues at position f form an excessively charged domain in peptides A and B, respectively. Incorporation of serine in peptide C results in a balanced distribution of charged residues. All three peptides have been investigated under different environmental conditions regarding conformational behavior and aggregate morphology.

pH dependence of folding: Circular dichroism (CD) spectroscopy was applied to investigate the secondary structure of all peptides at three selected pH values: 4.0, 7.4, and 9.0 (Figure 2). During the measurements, it was seen that peptides A and B require sufficient concentration to adopt a defined conformation. Below this concentration limit, which was 300 and 170 μM for peptides A and B, respectively, random coil structures were observed throughout (e.g., 250 μM peptide A at pH 4.0, see Figure SE1 in the Supporting Information).[19] In contrast, no concentration limit was detected for peptide C, even at concentrations below 50 μM.

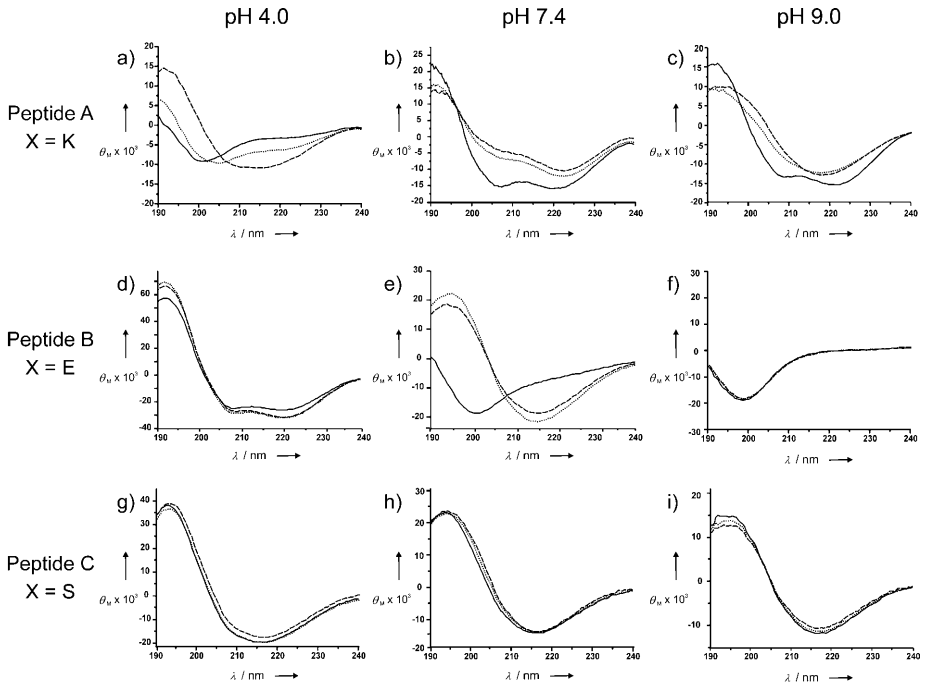

Figure 2. Representative CD spectra of a–c) peptide A (600 μM), d–f) peptide B (200 μM), and g–i) peptide C (50 μM) under acidic (10 mM acetate buffer, pH 4.0), neutral (10 mM Tris/HCl buffer, pH 7.4), and basic conditions (10 mM glycine/NaOH buffer, pH 9.0). The spectra were recorded after 0 (solid line), 24 (dotted line), and 72 h (dashed line) of incubation.

To maintain comparability between the different pH values, the concentration of each individual peptide was kept constant and above the respective limit. Figure 2 shows the obtained CD spectra recorded immediately after sample preparation (0 h), after 24 h of incubation, and after 72 h of incubation when all the spectra became invariable.

At pH 4.0 and concentrations above 300 μM, peptide A showed a slow transition from random coil to β-sheet, which is indicated by the evolving minimum at $\lambda = 216$ nm in the CD spectrum (Figure 2a).[19] At pH 7.4, peptide A adopted an α-helical conformation according to the characteristic CD minima at $\lambda = 222$ and 208 nm (Figure 2b). Followed over several days, the signal in the CD spectra remained α-helical, although the $[\theta]_{208}/[\theta]_{222}$ peak ratio became increasingly smaller. A similar effect was observed for other aggregating peptide systems[21] and might be ascribed to enhanced light scattering because of the growth of aggregates. Surprisingly, peptide A shows a rapid transition to a β-sheet structure at pH 9.0, although a helical conformation is observed as the initial structure (Figure 2c). Unlike peptide A, peptide B already folds into a defined conformation at a perceptibly lower concentration of about 170 μM. However, regarding the conformational preferences, an almost complementary behavior was observed. Peptide B adopted an α-helical conformation at pH 4.0 (Figure 2d), whereas a neutral pH value induces a transition from random coil to β-sheet (Figure 2e). At basic pH values, no defined conformation was found, even if the concentration was increased up to 1 mM (Figure 2f). In contrast to peptides A and B, peptide C did not respond to a changed pH value. Typical β-sheet CD signatures were found immediately after dissolution, independent of the peptide concentration and pH value (Figure 2g–i).

Comparing the results of all three peptides shows that the simultaneous substitution of only two amino acid residues at position f within the heptad repeat with lysine, glutamate, or serine causes a highly diverse pH-dependent folding behavior. Peptide A adopts a stable helical structure under physiological conditions with the pH switch in the OFF state, whereas an excessively charged domain of lysine residues (positions b, e, and f) destabilizes the α-helical structure at pH 4.0. Under these conditions, the pH switch is in the ON state and β-sheet-rich amyloid-like assemblies are formed as a consequence. Interestingly, there is no indication for unfolding of peptide A at pH 9.0. Here, a typical α-helical signature signal in the CD spectra was obtained directly after dissolution of the peptide. Although the pH switch is in the OFF state, a time-dependent transition into a β-sheet-rich structure is observed within 24 hours of incubation. Thus, it appears that the competing helical structure, which is present for the freshly prepared solution, is not sufficiently dominant to prevent a conversion into amyloid-like structures. A lower helix stability caused by charge repulsions between glutamate residues at positions c and g might be a possible explanation for this unexpected behavior.

The replacement of two lysine residues at position f by glutamate in peptide B yields a partially reversed pH dependence of folding, which was expected from the design. Helical structures are formed under acidic conditions in which the pH switch is in the OFF state, whereas a slow association into amyloid-like species is observed at neutral pH with the switch in the ON state. Compared to peptide A, peptide B exhibits a domain with a decrease in lysine residues (positions b and e), and repulsions between these residues are no longer strong enough to destabilize the α-helical structure at pH 4.0. An excessively charged domain of glutamic acid residues (positions c, f, and g), on the other hand, destabilizes the α-helical coiled-coil conformation under neutral conditions, which results in unfolding and a consecutive association into amyloid-like assemblies. Analogous to pH 7.4, peptide B does not fold into a defined conformation at pH 9.0. However, in contrast to neutral pH, this unor-

dered structure is maintained for the entire observation period of three days and no amyloid-like structures are formed. A basic pH value seems to additionally disrupt the β-sheet structure by Coulomb repulsions.

Peptide C forms β-sheet-rich species at all three pH values, although the extent of similarly charged domains is limited to positions c/g and b/e. Removing the excessively charged domain by incorporation of serine at position f apparently changes two parameters at once, that is, the charge state and the overall secondary structure propensity of the system. Both lysine and glutamic acid possess comparable α-helix and β-sheet propensities and can therefore be exchanged to evaluate the design principles.[22,23] However, serine exhibits a perceptibly lower α-helix propensity, which presumably affects the overall amyloid-formation propensity of the peptide.[22,23] Thus, the design of peptide C does not allow sufficient validation of the applied principles of intramolecular-charge repulsions as a switch to control amyloid formation.

pH dependence of peptide assembly: Transmission electron microscopy (TEM) was used to obtain information on the aggregate morphology of the different peptide samples investigated by CD spectroscopic analysis. The results are given with regard to the observed type of secondary structure.

Samples of unfolded peptides (e.g., peptide B at pH 9.0; Figure 3f) show small particles with a typical size of 2.5–3.5 nm. This size is in good agreement with the theoretical diameter of a single solvated peptide molecule.[19] In the case of an α-helical conformation of peptide A at pH 7.4, cryo-TEM studies reveal extended and rather stiff fibrils with total lengths in the micrometer range and a uniform diameter of (2.5 ± 0.3) nm (Figure 3b). Up to a peptide concentration of 1 mM, this uniform morphology remains unchanged. Further investigations on the ultrastructure of peptide B at pH 4.0 (Figure 3d) reveal fibers that are not distinguishable from those of peptide A at pH 7.4.[19] So far, we have not been able to gain any experimental evidence on the internal packing of α-helices within these fibers, but others have spent much effort to characterize α-helical fibers by CD, TEM, and X-ray fiber diffraction studies.[21,24–26] An arrangement that consists of single α helices that are staggered along the fiber axis in the sense of a superhelix has been proposed for these fibrils. On the basis of this structural model and the fiber diameter estimated from the present cryo-TEM data, a three- or four-strand fiber cross-section can be assumed for peptides A and B.

Numerous investigations have shown that β-sheet-rich amyloid fibrils exhibit multiple distinct morphologies, which are described as twisted or parallel assemblies of individual protofilaments.[27–29] For peptide A at pH 4.0, a mixture of fibril morphologies is generally observed that consists of twisted ribbons of a width of approximately 10 nm and tubular structures (Figure 3a). For larger fibrils, the revealed ultrastructure clearly points to a laterally packed assembly of thin protofilaments with an estimated thickness of approximately 3.5 nm (see Figure SA1 in the Supporting Information). Similar protofilament dimensions and the characteristic amyloid packing reflexes at 0.47 and 1.0 nm were additionally observed for peptide A (see Figure SB1 in the Supporting Information).[30] Despite this enormous amount of data, it is so far not clear how peptide A molecules are arranged within the protofilaments. A fully extended conformation as assumed previously[19] can definitely be excluded because the molecule contour length of 9.1 nm exceeds the diameter of the protofilament many times. To match a protofilament diameter of 3.5 nm, peptide A has to be bent at least once, which makes a hairpin- or sandwich-like internal

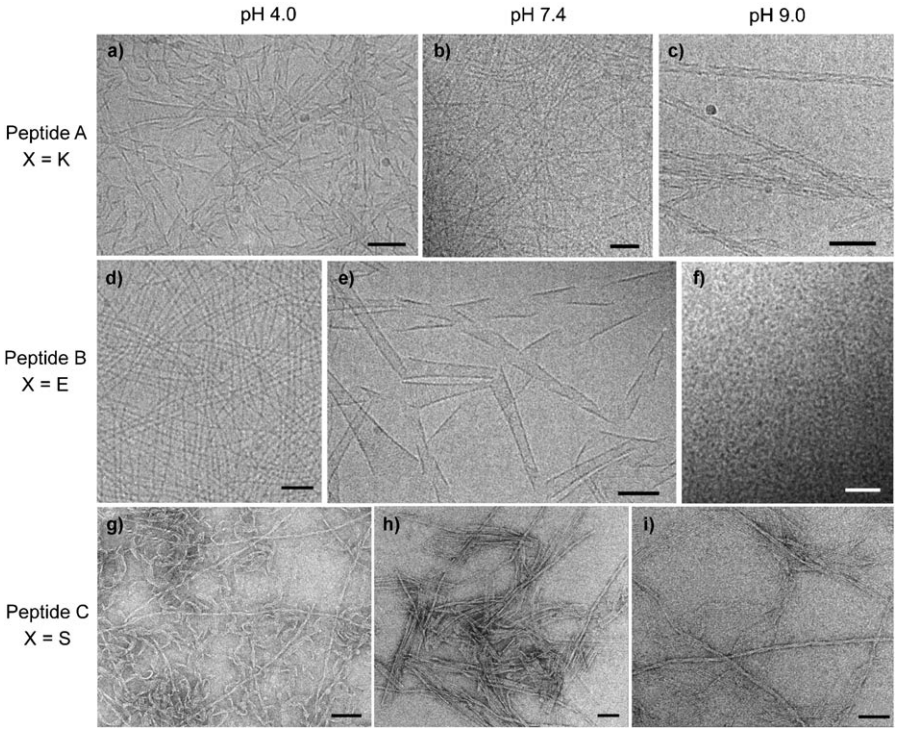

Figure 3. Cryo-TEM images of peptide A (500 μM) at a) pH 4.0, b) pH 7.4, and c) pH 9.0; peptide B at d) pH 4.0 (200 μM), e) pH 7.4 (375 μM), and f) pH 9.0 (1 mM). TEM images of PTA-stained fibrils of peptide C (300 μM) at g) pH 4.0, h) pH 7.4, and i) pH 9.0. The samples were prepared in 10 mM buffer solution (acetate buffer, pH 4.0; Tris/HCl buffer, pH 7.4; glycine/NaOH buffer, pH 9.0). Scale bars: 50 nm (a, c, e, g, h, i), 30 nm (b, d, f).

organization more likely. Further suggestions on the internal structure would be merely speculative without additional experimental data. Solid-state NMR spectroscopic and proline-scanning experiments to address this problem are currently in progress.

Although peptide A adopts a similar conformation at pH 4.0 and 9.0, the overall morphologies differ. At pH 9.0, the fibrils display a rather homogeneous and stiff appearance by several hundreds of nanometers in length. The small diameter of only approximately 10 nm suggests that those fibrils are composed of only a few protofilaments (Figure 3c). For peptide B at pH 7.4, different coexisting morphologies have again been observed. Helically twisted ribbons of variable width, giant cylinders, and funnel-like structures can be found (Figure 3e). In contrast to peptide A, all of these structures very clearly show the constituent protofilaments (see Figure 3e and Figures SA2 and SA3 in the Supporting Information) with a diameter of (3.5 ± 0.2) nm. Peptide C shows two types of fibrils (see Figure 3g and Figure SA4 in the Supporting Information) at pH 4.0. The first fibril is coiled and rather stiff, presumably consisting of a pair of approximately 3.5 nm thin protofilaments. The second fiber motif has a curly appearance and is usually composed of three or four protofilaments that are laterally assembled. These curly fibrils disappear completely at pH 7.4. Instead, relatively stiff ribbon-like fibrils composed of 5–10 protofilaments prevail against some coiled fibrils with a slightly increased diameter (Figure 3h). A further increase of the pH value to 9.0 yields an unchanged gross morphology for peptide C (Figure 3i).

Fibril-growth kinetics: Since the early years of amyloid research, it has been known that several dyes such as Congored (CR) and Thioflavin T (ThT) bind to amyloid-like structures more or less specifically.[31] In the case of ThT, this binding is accompanied by an enhanced fluorescence emission at $\lambda=482$ nm when excited at $\lambda=450$ nm, whereas CR shows a typical apple-green birefringence under polarized light. Although the exact binding mechanisms remain unclear to date,[32,33] ThT-binding assays have especially evolved as the most widely used tool to study the kinetics of amyloid formation. In general, two different assembly routes are discussed in the literature: 1) a two-step process that consists of a slow nucleation step followed by rapid fibril elongation[34] and 2) a non-nucleation-dependent pathway of rapid growth with the initial lag phase missing.[29,35,36] To compare the fibril-growth kinetics of all three peptides, we carried out ThT-binding studies under pH conditions at which amyloid-like aggregates are formed. Both, peptide A at pH 4.0 and peptide B at pH 7.4 show a similar sigmoidal increase in ThT fluorescence. Thus, peptides A and B assemble into amyloid-like structures by following a typical nucleation-dependent aggregation pathway (Figure 4a). A comparison of the calculated midpoint times reveals a faster fibril formation of peptide B that is consistent with the progress of conformational transformation monitored by CD spectroscopic analysis (Figure 2a and 2e).

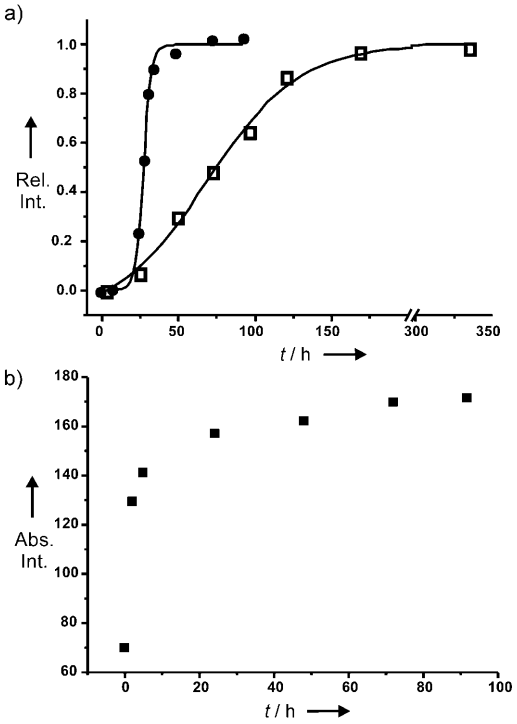

Figure 4. ThT-staining assay of a) peptide A (600 μM) at pH 4.0 (□), peptide B (200 μM) at pH 7.4 (●), and b) peptide C (200 μM) at pH 7.4 (■) at 25 °C. For both peptides A and B, the normalized fluorescence intensity was fit to a sigmoidal growth model (see the Experimental Section). The midpoint times of aggregation of peptides A and B are 69 and 27 h, respectively.

In contrast, no lag time could be detected for peptide C at pH 7.4 (Figure 4b). The ThT-binding assay rather points to a non-nucleation-dependent fibril formation. These findings correspond to the CD data in which no structural transition was observed (Figure 2h). It is known that the nucleation-dependent aggregation is thermally activated.[37,38] Therefore, the temperature was decreased to 4 °C in an additional experiment to ensure that the fast kinetics of fibril formation at 25 °C do not hinder the detection of any lag time. Also under these conditions, the fluorescence emission does not exhibit any lag time, thus supporting a non-nucleated pathway (see Figure SC1 in the Supporting Information). However, the data of peptide C at 25 °C could not be fitted adequately to a single-exponential function that is generally used to describe non-nucleation-dependent fibril formation.[36] Therefore, neither the nucleation-dependent nor the rather rarely described non-nucleation-dependent pathways can be excluded on the basis of the given results. Further measurements are needed to draw an unambiguous conclusion.

Ionic-strength variations: Controllable intrahelical electrostatic repulsions are a key issue of the design presented herein. Under certain conditions, these repulsions should prevent helical folding and as a consequence promote amyloid formation. As mentioned previously, the design of peptide C does not allow sufficient validation of our concept of

intramolecular-charge repulsions as a switch to control amyloid formation, because the substitution of lysine or glutamic acid residues by serine in peptide C additionally affects the overall amyloid-formation propensity of the system. However, interhelical[39] and intrahelical[40] Coulomb repulsions between amino acid side chains in coiled coils can be diminished by the presence of charged co-solutes. Sufficient screening of charges should therefore facilitate a helical folding, also under conditions in which peptides A, B, and C remain unfolded or convert into amyloid-like assemblies. Consequently, various salts were added under different concentrations to further elucidate and validate the role of intrahelical charge repulsions in regard to the design.

It is not only the valency of salt ions that determines their ability to accommodate the forces between charged objects. Specific ion effects are well documented as well.[41] With a focus on protein folding, ions are usually classified regarding size and charge density into strongly and weakly hydrated ions, so-called kosmotropes (water-structure makers) and chaotropes (water-structure breakers), respectively.[42] For ion-pair formation, kosmotrope/kosmotrope and chaotrope/chaotrope pairs are preferred. Similar to other nitrogen-based cations, lysine side chains are chaotrope, whereas carboxy-functionalized glutamic acid side chains are a typical kosmotrope (Figure 5).[42] From the design and the observed

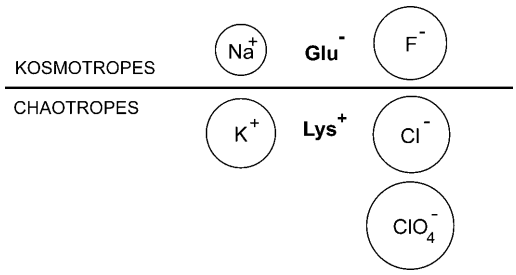

Figure 5. Classification of selected cations, anions, lysine and glutamic acid into kosmotropes and chaotropes (modified according to ref. [42]). In comparison with the Cl^- ion, the higher distance to the dividing line of the ClO_4^- ion indicates a stronger chaotropic character.

conformational behavior, we assume that Coulomb repulsions between Glu/Glu and Lys/Lys cause the gained pH specificity. To effectively screen both types of ionic repulsions at once, a specific salt that consists of a kosmotropic cation (to match glutamate) and a chaotropic anion (to match lysine) would be required. On the other hand, only an insufficient charge-screening effect would be expected for salts that do not fulfill this requirement. Therefore, $NaClO_4$, NaCl, and KF were selected for the following investigations.

As a result of the equal number of positively and negatively charged residues, which are both charged under neutral pH conditions, peptide C represents an ideal system to search for specific ion effects. Thus, peptide C at pH 7.4 was investigated in the presence of different amounts of the selected cation/anion pairs by using CD spectroscopy (Figure 6). Regardless of the kosmotropic or chaotropic nature of the ions, no significant effect on the conformation was observed in presence of 1 M salt (see Figure SE2 in the

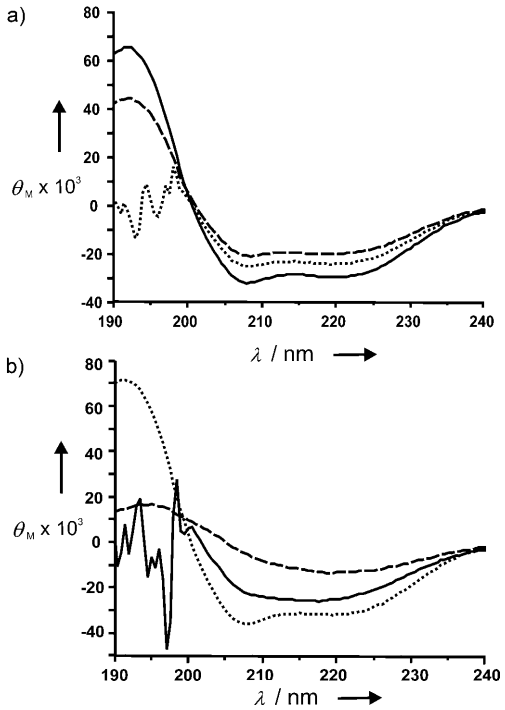

Figure 6. Peptide C (50 μM, 10 mM Tris/HCl buffer, pH 7.4) in the presence of 3 M NaCl (solid line), $NaClO_4$ (dotted line), or KF (dashed line) after a) 1 and b) 72 h of incubation.

Supporting Information). At a concentration of 3 M, all salts induce a clear α-helical coiled-coil structure immediately after dissolution of the peptide (Figure 6a). However, this structure survived an incubation time of 72 hours only in the presence of $NaClO_4$, whereas a clear conformational transition to a β-sheet-rich structure occurs in the case of KF (Figure 6b). Incubation in the presence of NaCl yielded ambiguous CD traces, which provide evidence for a mixed conformation that contains fractions of helical and sheet structures.

The distinct conformations observed for peptide C within 72 hours of incubation point to perceptible differences in the charge-accommodating ability of the investigated salts. β-sheet formation was fully inhibited only in the presence of $NaClO_4$, whereas explicit structural changes were observed for NaCl and KF. A reasonable explanation for this behavior can be obtained by comparison of the nature of the involved ion (Figure 5). As mentioned above, charged glutamic acid side chains are kosmotropic and can therefore be screened efficiently by Na^+ ions, which form a kosmotrope/kosmotrope ion pair. In contrast, K^+ ions are rather chaotropic and consequently do not match the kosmotropic carboxy functionalities of glutamate. Thus, the Na^+ ion is the preferred cation to diminish ionic repulsions in the negatively charged domain of peptide C. Positively charged lysine

side chains, on the other hand, are a typical chaotrope and therefore require a chaotropic anion. The chloride ion is neither a typical chaotrope nor a kosmotrope and the fluoride ion acts strongly kosmotropic. Out of the investigated anions, only the ClO_4^- ion exhibits a clear chaotropic nature. NaCl and KF are therefore only able to form the required matching ion pairs with either lysine or glutamate residues, but not with both at once. As a consequence, either the positively or negatively charged domains in peptide C are not sufficiently screened, which accordingly results in a slow structural transition from an α-helix to a β-sheet. In contrast, $NaClO_4$ has the potential to screen both the positively and negatively charged domains. As a result, a stable α-helical conformation is maintained after 72 hours of incubation and, more importantly, the structural transition into a β-sheet-rich structure is inhibited.

From these results, the question arose if there is a correlation between the stability of the initially formed, salt-induced α-helix and the tendency of the peptides to time-dependently assemble into amyloid-like structures. To clarify this question, thermal denaturation profiles of peptide C in the presence of the three different salts were recorded by CD spectroscopic analysis (see Figure SD1 in the Supporting Information). The measurements were started immediately after sample preparation when all peptide solutions were still α-helical (Figure 6a). Roughly identical midpoint temperatures T_m of 38 and 36 °C were obtained for NaCl and KF, respectively. In contrast, peptide C exhibits much higher α-helix stability with a perceptibly elevated melting point of $T_m \approx 58$ °C when incubated with $NaClO_4$. Apparently, there is indeed a correlation between coiled-coil stability and amyloid-formation propensity for peptide C, thus further validating the existence of two folding motifs that are competing with each other.

Besides peptide C, peptides A and B were also investigated in the presence of 3 M $NaClO_4$ at concentrations and pH values at which they usually do not adopt a defined conformation (peptides A and B) or assemble into amyloids (peptide C). Figure 7 exemplarily shows CD traces of 50 μM peptide A at pH 4.0 and 50 μM peptide B and C at pH 7.4 after incubation with 3 M $NaClO_4$ for 72 h. In the absence of $NaClO_4$, peptide A does not fold into a defined conformation.[19] In contrast, a clear helical structure, which was maintained for three days, was obtained in the presence of salt (Figure 7, solid line). Similar helix-inducing effects of $NaClO_4$ were observed for peptide B at pH 7.4 and three days of incubation (Figure 7, dotted line). These results clearly show that a $NaClO_4$-mediated screening of ionic repulsions also yields helical structures for peptides A and B. This finding further confirms the crucial role of electrostatic repulsions for the presented design.

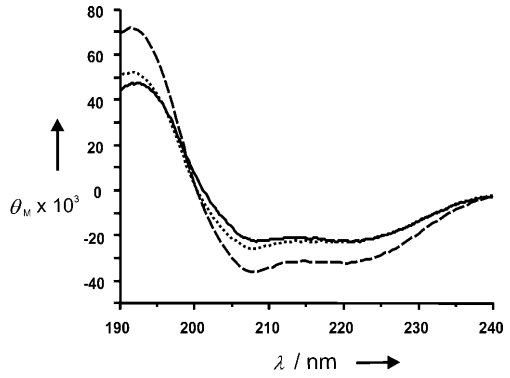

Figure 7. CD spectra of 50 μM peptide A (solid line) at pH 4.0 and 50 μM peptides B (dotted line) and C (dashed line) at pH 7.4 after 72 h in the presence of 3 M $NaClO_4$.

Nevertheless, it is important to mention that all peptides slowly assemble into β-sheet-rich structures with 3 M $NaClO_4$ and at peptide concentrations that are considerably higher than 50 μM (e.g., peptide C at 95 μM; see Figure SE3 in the Supporting Information). This behavior is hardly surprising because an enormous increase in the overall amyloid-formation tendency of the system at elevated concentrations was also observed in the absence of salt. Additionally, amyloid formation in general is known to be a highly concentration-dependent process.[6] Thus, it can be assumed that the salt-mediated coiled-coil conformation above a certain concentration does not provide enough stability to sufficiently compete with the urge of the system to convert into amyloids.

Conclusion

We present a series of three simplified amyloid-forming model peptides that, depending exclusively on concentration and pH value, adopt different conformations and fibril morphologies. These de novo designed peptides strictly follow the characteristic heptad repeat of the α-helical coiled-coil folding motif. The two characteristic coiled-coil recognition motifs have been designed to deliver maximum stability and were maintained optimized to provide an intrinsic ability for a helical folding. Furthermore, two types of modifications were incorporated at solvent-exposed positions within the heptad repeat. First, β-sheet preferring valine residues were inserted to make the system prone to amyloid formation. Second, charged glutamic acid or lysine residues were placed adjacently at one side of the helical cylinder, thus forming an excessively charged domain that serves as a pH switch. The resulting model system consequently exhibits structural features of both α-helical coiled-coil folding and amyloid formation, and changes in pH value or concentration can be used to direct these ambiguous conformational preferences in either direction. Intermolecular charge repulsions in the ON state of the pH switch lead to a destabilization of the competing helical conformation, which results in the formation of amyloid-like assemblies at a sufficient peptide concentration. Contrarily, the OFF state of the pH switch yields non-amyloidogenic α-helical fibrils.

Whereas other approaches obligatorily require elevated temperatures to control coiled-coil-to-amyloid transitions, the design reported herein exclusively requires alterations in pH value and/or concentration. The presented model pep-

tides therefore represent an ideal system to directly follow amyloid-formation processes under native-like conditions by applying high-resolution methods such as NMR spectroscopy. Additionally, there is increasing interest in applying amyloid-like structures as novel biomaterials.[43,44] The described design generates a highly pH-specific conformational behavior and consequently represent a promising tool which can be used to control and direct-assembly processes in materials science.

Experimental Section

Peptide synthesis and purification: Peptides were synthesized by solid-phase assembly on Fmoc-Leu-OWang resin (0.65 mmol g^{-1}) using the Fmoc strategy and a Multi-Syntech Syro XP peptide synthesizer (Multi-synTech GmbH, Witten, Germany). To determine the concentration by UV/Vis spectroscopic analysis, the peptides were N-terminally labeled with anthranilic acid (Abz). The peptides were cleaved from the resin by reaction with 4 mL of a solution containing 10% (w/v) triisopropylsilane, 1% (w/v) water, and 89% (w/v) trifluoroacetic acid (TFA). The crude peptides were purified by reversed-phase HPLC on a Knauer smartline manager 5000 system (Knauer GmbH, Berlin, Germany) equipped with a C8 (10 μm) LUNA Phenomenex column (Phenomenex Inc., Torrance, CA, USA). Peptides were eluted with a linear gradient of acetonitrile/water/0.1% TFA (see Chapter F in the Supporting Information) and identified by using MALDI-TOF mass spectrometry (MS). All MS analyses were performed on a Bruker Reflex III spectrometer. Peptide purity was determined by analytical HPLC on a Merck LaChrom system (Merck KGaA, Darmstadt, Germany) equipped with a C8 (10 μm) LUNA Phenomenex column (Phenomenex Inc., Torrance, CA, USA). The gradients used were similar to those of the preparative HPLC.

Sample preparation: The peptide solutions were prepared in freshly filtered acetate buffer (10 mM, pH 4.0), Tris/HCl buffer (10 mM, pH 7.4), and glycine/NaOH buffer (10 mM, pH 9.0), respectively. The nature of the buffer salts had no effect on the results; only ionic strength and the pH value affected the secondary structure of the peptides. Fibrils were formed at 20 °C without further shaking. The peptide concentration was calculated by comparing the absorbance at $\lambda = 320$ nm with a calibration curve determined by the absorbance of Abz–glycine at different concentrations in the corresponding buffer. Structure formation was checked by CD spectroscopic analysis over 2 weeks and is shown for different incubation times (0, 24, and 72 h).

CD spectroscopy: CD spectra were recorded on a J-810 spectropolarimeter (Jasco GmbH, Gross-Umstadt, Germany) at 20 °C. Quartz cells with 0.2- and 0.5-mm path lengths were used for higher (>200 μM) and lower (<200 μM) peptide concentrations, respectively. The spectra were the average of three scans obtained by collecting data from 190 to 240 nm at 0.2-nm intervals, 2-nm bandwidth, and 1-s response time. In each case, buffer spectra were also collected and subtracted from the peptide spectra. The measured CD data in mdeg were converted into molar ellipticities per residue $[\theta]$ using Origin software (version 7.0, Microcal, USA).

TEM: Aliquots (6 μL) of peptides in solution were absorbed for 1 min to glow-discharged carbon-coated collodium films on 400-mesh copper grids. After blotting and negative staining with 1% phosphotungstic acid (PTA) or 1% uranyl acetate (UAc) the grids were air-dried. Micrographs were taken at primary magnification of 58300× using a defocus of 0.6 μm. The samples for cryo-TEM were prepared by placing a droplet (10 μL) of the solution on a hydrophilized (60-s plasma treatment at 8 W using a BALTEC MED 020 device) perforated carbon-filmed grid (Qantifoil, Jena, Germany) at room temperature. The supernatant fluid was removed with filter paper until an ultrathin layer of the sample solution was obtained spanning the holes of the carbon film. The grids were immediately vitrified in liquid ethane at its freezing point (−184 °C) using a standard plunging device. The vitrified samples were transferred under liquid nitrogen into a Philips CM12 transmission electron microscope using the Gatan cryo holder and stage (model 626). Microscopy was carried out at a sample temperature of −175 °C by using the low-dose protocol of the microscope at a primary magnification of 58300×. The defocus was chosen to be 1.5 μm in all cases.

ThT assay: ThT (obtained from Sigma Aldrich) was purified by reverse-phase column chromatography. Fluorescence spectra were measured with a luminescence spectrometer LS 50B (The Perkin Elmer Cooperation, Boston, MA, USA). Because of the poor binding of ThT to amyloids at pH 5.0 or below, peptide solutions were allowed to fold into β-sheet structures under the appropriate pH conditions, also including pH 4.0, and were threefold diluted with Tris/HCl buffer (10 mM) to pH 7.4 with a final molar peptide/ThT ratio of 4:1 for the ThT assay. The samples were allowed to incubate for 30 min at room temperature. The spectra were collected in quartz cells with a 10-mm path length between $\lambda = 470$ and 600 nm after excitation at $\lambda = 450$ nm. The slit width of excitation and emission monochromators was set to 10 and 15 nm, respectively. Kinetic aggregation traces were generated from time traces of ThT fluorescence intensity at $\lambda = 482$ nm and corrected for the contribution of the free dye. The measured fluorescence intensity values for peptides A and B are given after normalization so that the final fluorescence intensity at the endpoint of the kinetic trace was 100%. For both peptides, the resulting plot of fluorescence intensity versus time was fitted by a sigmoidal equation: $FL = a + (b-a)/\{1+\exp[r(t-t_m)]\}$ using Origin software (version 7.0, Microcal, USA), where FL is the normalized ThT fluorescence intensity, a and b are the plateau values, t is time, t_m is the midpoint time, and r is a growth rate. The squared correlation coefficient R^2 was greater than 0.995.

Thermal denaturation: Each peptide solution (50 μM in 10 mM Tris/HCl buffer, pH 7.4) was treated with 3 M guanidine hydrochloride (GdnHCl) as a denaturant to ensure complete denaturation by increasing the temperature to 90 °C and loaded into a quartz cell with a 1.0-mm path length. CD spectra were measured in intervals of 0.5 °C from 20 to 90 °C with a heating rate of 5 °C min^{-1}. For each peptide, the data were converted into the molar fraction of unfolded peptide (f_u), according to the equation: $f_u = ([\theta]-[\theta]_n)/([\theta]_u-[\theta]_n)$, where $[\theta]$ is the observed molar ellipticity per residue at $\lambda = 222$ nm and $[\theta]_n$ and $[\theta]_u$ are the mean residue ellipticities of the native (folded) and denatured (unfolded) states, respectively. The molar fraction of unfolded peptide was plotted against temperature and fitted by using a sigmoidal equation. For quantitative comparison of helical stability, the midpoint temperature T_m, at which 50% of the peptide remains folded, was determined.

Acknowledgements

This study was supported by the Deutsche Forschungsgemeinschaft DFG (projects KO 1976/5–1 and BO 1000/7–1) and the Freie Universität Berlin. S.C.W. thanks the Fonds der Chemischen Industrie for financial support.

[1] J. W. Kelly, *Curr. Opin. Struct. Biol.* **1996**, *6*, 11–17.
[2] M. Stefani, C. M. Dobson, *J. Mol. Med.* **2003**, *81*, 678–699.
[3] J. I. Guijarro, M. Sunde, J. A. Jones, I. D. Campell, C. M. Dobson, *Proc. Natl. Acad. Sci. USA* **1998**, *95*, 4224–4228.
[4] O. S. Makin, L. C. Serpell, *FEBS J.* **2005**, *272*, 5950–5961.
[5] M. R. Sawaya, S. Sambashivan, R. Nelson, M. I. Ivanova, S. A. Sievers, M. I. Apostol, M. J. Thompson, M. Balbirnie, J. J. W. Wiltzius, H. T. McFarlane, A. O. Madsen, C. Riekel, D. Eisenberg, *Nature* **2007**, *447*, 453–457.
[6] I. W. Hamley, *Angew. Chem.* **2007**, *119*, 8274–8295; *Angew. Chem. Int. Ed.* **2007**, *46*, 8128–8147.
[7] J. W. Kelly, *Proc. Natl. Acad. Sci. USA* **1998**, *95*, 930–932.
[8] M. T. Pastor, A. Esteras-Chopo, M. L. de la Paz, *Curr. Opin. Struct. Biol.* **2005**, *15*, 57–63.
[9] Y. B. Yu, *Adv. Drug Delivery Rev.* **2002**, *54*, 1113–1129.
[10] J. M. Mason, K. M. Arndt, *ChemBioChem* **2004**, *5*, 170–176.
[11] D. N. Woolfson, *Adv. Protein Chem.* **2005**, *70*, 79–112.

[12] Y. Takahashi, A. Ueno, H. Mihara, *Chem. Eur. J.* **1998**, *4*, 2475–2484.
[13] Y. Takahashi, A. Ueno, H. Mihara, *Bioorg. Med. Chem.* **1999**, *7*, 177–185.
[14] B. Ciani, E. G. Hutchinson, R. B. Sessions, D. N. Woolfson, *J. Biol. Chem.* **2002**, *277*, 10150—10155.
[15] R. A. Kammerer, D. Kostrewa, J. Zurdo, A. Detken, C. Garcia-Echeverria, J. D. Green, S. A. Muller, B. H. Meier, F. K. Winkler, C. M. Dobson, M. O. Steinmetz, *Proc. Natl. Acad. Sci. USA* **2004**, *101*, 4435–4440.
[16] H. Dong, J. D. Hartgerink, *Biomacromolecules* **2007**, *8*, 617–623.
[17] M. O. Steinmetz, Z. Gattin, R. Verel, B. Ciani, T. Stromer, J. M. Green, P. Tittmann, C. Schulze-Briese, H. Gross, W. F. van Gunsteren, B. H. Meier, L. C. Serpell, S. A. Muller, R. A. Kammerer, *J. Mol. Biol.* **2008**, *376*, 898–912.
[18] K. Pagel, T. Seri, H. von Berlepsch, J. Griebel, R. Kirmse, C. Böttcher, B. Koksch, *ChemBioChem* **2008**, *9*, 531–536.
[19] K. Pagel, S. C. Wagner, K. Samedov, H. von Berlepsch, C. Böttcher, B. Koksch, *J. Am. Chem. Soc.* **2006**, *128*, 2196–2197.
[20] X. I. Ambroggio, B. Kuhlman, *Curr. Opin. Struct. Biol.* **2006**, *16*, 525–530.
[21] M. J. Pandya, G. M. Spooner, M. Sunde, J. R. Thorpe, A. Rodger, D. N. Woolfson, *Biochemistry* **2000**, *39*, 8728–8734.
[22] P. Y. Chou, G. D. Fasman, *Biochemistry* **1974**, *13*, 222–245.
[23] P. Y. Chou, G. D. Fasman, *Annu. Rev. Biochem.* **1978**, *47*, 251–276.
[24] S. A. Potekhin, T. N. Melnik, V. Popov, N. F. Lanina, A. A. Vazina, P. Rigler, A. S. Verdini, G. Corradin, A. V. Kajava, *Chem. Biol.* **2001**, *8*, 1025–1032.
[25] T. N. Melnik, V. Villard, V. Vasiliev, G. Corradin, A. V. Kajava, S. A. Potekhin, *Protein Eng.* **2003**, *16*, 1125–1130.
[26] D. Papapostolou, A. M. Smith, E. D. T. Atkins, S. J. Oliver, M. G. Ryadnov, L. C. Serpell, D. N. Woolfson, *Proc. Natl. Acad. Sci. USA* **2007**, *104*, 10853–10858.
[27] C. S. Goldsbury, G. J. Cooper, K. N. Goldie, S. A. Muller, E. L. Saafi, W. T. Gruijters, M. P. Misur, A. Engel, U. Aebi, J. Kistler, *J. Struct. Biol.* **1997**, *119*, 17–27.
[28] T. Stromer, L. C. Serpell, *Microsc. Res. Tech.* **2005**, *67*, 210–217.
[29] R. Kodali, R. Wetzel, *Curr. Opin. Struct. Biol.* **2007**, *17*, 48–57.
[30] H. von Berlepsch, R. R. Araghi, E. Brandenburg, K. Pagel, J. Leiterer, F. Emmerling, A. Schulz, C. Böttcher, B. Koksch, unpublished results.
[31] C. Wu, Z. Wang, H. Lei, W. Zhang, Y. Duan, *J. Am. Chem. Soc.* **2007**, *129*, 1225–1232.
[32] M. R. H. Krebs, E. H. C. Bromley, A. M. Donald, *J. Struct. Biol.* **2005**, *149*, 30–37.
[33] M. Groenning, M. Norrman, J. M. Flink, M. van de Weert, J. T. Bukrinsky, G. Schluckebier, S. Frokjaer, *J. Struct. Biol.* **2007**, *159*, 483–497.
[34] J.-C. Rochet, P. T. Lansbury, *Curr. Opin. Struct. Biol.* **2000**, *10*, 60–68.
[35] W. S. Gosal, I. J. Morten, E. W. Hewitt, D. A. Smith, N. H. Thomson, S. E. Radford, *J. Mol. Biol.* **2005**, *351*, 850–864.
[36] G. Plakoutsi, F. Bemporad, M. Calamai, N. Taddei, C. M. Dobson, F. Chiti, *J. Mol. Biol.* **2005**, *351*, 910–922.
[37] Y. Kusumoto, A. Lomakin, D. B. Teplow, G. B. Benedek, *Proc. Natl. Acad. Sci. USA* **1998**, *95*, 12277–12282.
[38] R. Sabaté, M. Gallardo, J. Estelrich, *Int. J. Biol. Macromol.* **2005**, *35*, 9–13.
[39] I. Jelesarov, E. Durr, R. M. Thomas, H. R. Bosshard, *Biochemistry* **1998**, *37*, 7539–7550.
[40] M. G. Oakley, P. S. Kim, *Biochemistry* **1998**, *37*, 12603–12610.
[41] M. Boström, D. R. Williams, B. W. Ninham, *Phys. Rev. Lett.* **2001**, *87*, 168103.
[42] K. D. Collins, *Biophys. J.* **1997**, *72*, 65–76.
[43] I. Cherny, E. Gazit, *Angew. Chem.* **2008**, *120*, 4128–4136; *Angew. Chem. Int. Ed.* **2008**, *47*, 4062–4069.
[44] H. Frauenrath, E. Jahnke, *Chem. Eur. J.* **2008**, *14*, 2942–2955.

Received: June 19, 2008
Revised: August 18, 2008
Published online: November 14, 2008

